This is a preprint of: "Analysis of unstable behavior in a mathematical model for erythropoiesis", Susana Serna, Jasmine A. Nirody, Miklos Z. Racz, *J. Math. Biol.*, vol. 66, 595–625, 2013.
DOI: [10.1007/s00285-012-0524-y]

Analysis of unstable behavior in a mathematical model for erythropoiesis

Susana Serna · Jasmine A. Nirody · Miklós Z. Rácz

Abstract We consider an age-structured model that describes the regulation of erythropoiesis through the negative feedback loop between erythropoietin and hemoglobin. This model is reduced to a system of two ordinary differential equations with two constant delays for which we show existence of a unique steady state. We determine all instances at which this steady state loses stability via a Hopf bifurcation through a theoretical bifurcation analysis establishing analytical expressions for the scenarios in which they arise. We show examples of supercritical Hopf bifurcations for parameter values estimated according to physiological values for humans found in the literature. Numerical simulations displaying the resulting oscillatory dynamics in agreement with the theoretical analysis are provided.

Keywords Age-structured model · Multiple delay differential equations · Hopf bifurcation · Erythropoiesis

1 Introduction

Dynamical diseases are characterized as those that occur through changes in the qualitative dynamics of physiological processes. This definition leads naturally to the description of dynamical diseases as a nonlinear system undergoing one or more bifurcations [21]. Indeed, mathematical models have proven to be an effective way to describe several dynamic pathologies [4,13,21,22,25,28]. In this paper, we focus on characterizing irregular dynamics of one specific physiological control system, the regulation of erythropoiesis via the feedback loop between erythropoietin and hemoglobin.

Erythropoiesis, the production of erythrocytes (red blood cells), involves interaction between two organ systems: the bone marrow, where the precursors to mature red blood cells are located, and the kidney, which produces the hormone erythropoietin. When the partial pressure of oxygen in the blood drops, suggesting hypoxia, specialized epithelial cells in the kidney release erythropoietin into the bloodstream. The erythropoietin then travels to the bone marrow where it both accelerates erythropoiesis and recruits additional stem cells into the committed pathway to become mature red blood cells.

Hemoglobin is an iron-containing metalloenzyme essential to erythropoiesis. Because a high percentage of the dry volume of a red blood cell consists of hemoglobin, low levels of this protein result in suboptimal red blood cell production regardless of erythropoietin release. On the other hand, high availability of hemoglobin allows for maximal levels of erythropoiesis. The function of hemoglobin is to act as a transport protein for oxygen in the bloodstream. For this reason, the increase in hemoglobin content (or red blood cell number) caused by elevated erythropoietin raises the oxygen carrying capacity of the blood and corrects hypoxia, thus removing the original pressure for the release of erythropoietin. This is an example of a negative feedback system, in which an excess of product suppresses its production. Many biological control systems involve negative feedback, and the disruption of such a loop can result in severe pathology [12, 15].

A mathematical model of hematopoiesis was introduced by Mackey [19], who proposed a model of two nonlinear differential equations with one constant delay representing the average cell cycle duration. Mackey's model is called an age-structured model, where populations are classified and tracked according to their age. Modifications of this model have been analyzed to be applied to a variety of hematological diseases by different authors, [2, 3, 6, 27]. Application of similar models to erythropoiesis can be found in [3, 5, 23]. For an extended review of past work, we refer to Foley and Mackey [12].

Many studies use bifurcation analysis to provide an understanding of the underlying system dynamics leading to pathology [16, 20]. Specifically, periodic diseases can be simulated by systems which undergo a Hopf bifurcation, a local bifurcation in which a limit cycle arises from an equilibrium point, resulting in oscillatory behavior [18, 29]. Such a bifurcation in a model of erythropoiesis would result in oscillatory behavior in both erythropoietin and hemoglobin levels [2, 4, 5]. In particular, this behavior has been observed in patients with renal failure treated with erythropoiesis-stimulating agents, or ESAs [11].

In this paper we consider a modification of the age structured model presented by Bélair et al. in [5] to describe red blood cell production. Since the total population of red blood cells actually consists of two distinct subpopulations, committed precursor cells and mature erythrocytes, the model analyzed in this paper implements two discrete delays corresponding to the lifespan of each of these subpopulations. We perform a complete theoretical bifurcation analysis to identify Hopf bifurcations. The derivation of analytical expressions which describe the conditions for which Hopf bifurcations occur provide a good understanding of how such models are relevant in reproducing oscillatory dynamics associated with dynamical diseases.

The paper is organized as follows. We introduce the mathematical model for regulation of erythropoiesis in Section 2. In Section 3, we perform a linear stability analysis after reducing the model to a system of ordinary differential equations with two discrete delays. We determine the unique equilibrium point of the system and derive the characteristic equation for the linearized system around this point. In Section 4 we

perform a bifurcation analysis providing a complete parameter study and determining the conditions for Hopf bifurcations. In this analysis, we demarcate three subregions of the parameter space under different conditions on the parameters, in which we demonstrate the existence of Hopf bifurcations. In this manner, we identify all possible Hopf bifurcations and establish analytical expressions for the scenarios in which they arise. We present simulations which provide examples of oscillatory dynamics resulting from Hopf bifurcations for physiologically relevant parameters in Section 5, and a concluding discussion in Section 6.

2 Model for regulation of erythropoiesis

In the process of erythropoiesis, new red blood cells are created from precursor cells in the bone marrow at a rate proportional to the amount of the hormone erythropoietin present in the body. These cells age over a period of months through abrasion in the capillaries, eventually losing all ability to transport oxygen, at which point they are destroyed by phage cells. Mature red blood cells carry hemoglobin, the concentration of which is fairly constant among the population of red blood cells and therefore a good measure of red blood cell levels. Erythropoietin and hemoglobin are involved in a negative feedback loop [14]. The mathematical model we consider for modeling these interactions is based on the age-structured system of equations introduced in [5].

Let t represent time and ν represent red blood cell age. Let $m(t,\nu)$ be the density of red blood cells in the body with respect to time t and red blood cell age ν. We assume that the cells age at a constant rate α, since the age of a red blood cell depends mainly on the number of times it passes through the capillary system. The level of hemoglobin $M(t)$ is determined as a proportion of the total density of red blood cells and influences the level of the hormone erythropoietin A(t). Consistent with the idea of negative feedback, the concentration of erythropoietin will decrease with increasing numbers of mature erythrocytes.

We describe the evolution of the red blood cell population by the transport equation

$$\frac{\partial m}{\partial t} + \alpha \frac{\partial m}{\partial \nu} = 0, \qquad \text{for} \quad \mathrm{t} \geq 0 \quad \text{and} \quad 0 \leq \nu \leq \nu_{\max}, \tag{1}$$

where $\nu_{\max}$ is the maximum age of a mature cell.

We impose the following time-dependent Dirichlet boundary condition

$$m(t,0) = \frac{1}{\alpha} E(A(t - T_{\mathrm{p}})), \tag{2}$$

where T_{p} is the time required for a stem cell committed to erythropoiesis to reach maturity, and E is a monotone increasing function that represents the rate of erythropoietin-driven production of red blood cells. We consider E to be a Hill function, as is common to enzyme kinetic models [7]. We express it as

$$E(s) = E_{\max} \frac{s}{s + E_{50}}, \quad \mathrm{s} \geq 0, \tag{3}$$

where $E_{\max}$ and E_{50} are the maximum concentration and pre-image of 50% saturation, respectively. This indicates that as the erythropoietin concentration increases, the amount of incoming red blood cells at time t increases as well, until it asymptotically reaches a saturation point. Note that there is a delay of time T_{p} in equation (2) due

to the time required for committed stem cells to mature fully. This delay signifies that the input at every time t is dependent on $A(t - T_{\mathrm{p}})$. We consider $A\,(t)$ to be known for $t \in [-T_{\mathrm{p}}, 0]$.

Since hemoglobin concentration is directly related to the total population of red blood cells, we have

$$M(t) = R \int_0^{\nu_{\max}} m(t, \nu)\ d\nu, \tag{4}$$

where R is a scaling constant representing the mean corpuscular hemoglobin—i.e. the amount of hemoglobin in a typical red blood cell.

We consider the negative feedback loop between the levels of hemoglobin $M(t)$ and erythropoietin $A(t)$. The time evolution of $A(t)$ is given by the differential equation

$$\frac{dA(t)}{dt} = -kA(t) + F(M(t)), \tag{5}$$

where $k > 0$ represents the elimination rate of erythropoietin, and we consider the rate of hemoglobin-driven production of erythropoietin F to be given by a decreasing Hill function

$$F(s) = F_{\max} \frac{{F_{50}}^r}{{F_{50}}^r + s^r}, \quad \mathrm{s} \geq 0, \tag{6}$$

where $F_{\max}$ and F_{50} are defined analogously to $E_{\max}$ and E_{50} in equation (3). The parameter r indicates the speed of response of the rate of hemoglobin-driven production to the level of hemoglobin. Consistent with the concept of negative feedback, an increase in hemoglobin concentration leads to a fall in the rate of erythropoietin production, as seen by the decrease of $F(M(t))$, and consequently of the left hand side of equation (5), as $M(t)$ rises.

We review the parameters we have introduced and their associated units in Table 1.

Table 1 Parameter values and associated units.

Parameter	Units
α	none
$\nu_{\max}$	day
T_{p}	day
k	day^{-1}
R	g
$E_{\max}$	$1/(\ell \cdot \mathrm{day})$
E_{50}	U/ℓ
$F_{\max}$	$\mathrm{U}/(\ell \cdot \mathrm{day})$
F_{50}	g/ℓ
r	none

The existence of Hopf bifurcations in similar models to the one we have presented have been suggested in different approaches [4,5,20]. In the following sections we determine the conditions for existence of Hopf bifurcations in the dynamics of the erythropoietin-hemoglobin regulation loop for the complete parameter space. In order to perform a bifurcation analysis we first present a linear stability analysis to determine the conditions under which the unique equilibrium point of the system can lose stability.

3 Linear stability analysis

The system introduced above consists of three equations describing red blood cell population (eq. (1)), hemoglobin levels (eq. (4)) and erythropoietin levels (eq. (5)). In this section we express the system as a pair of ordinary differential equations with two delays. Such a reduction is natural as it allows us to concentrate on the feedback loop between rates of erythropoietin and hemoglobin production. We then show the existence of a unique, physiologically relevant equilibrium point, and analyze the stability of the system linearized around this point.

3.1 Reduction to a system of ordinary differential equations with delay

We first use the method of characteristics to solve the transport equation (1). The directional derivative of m along the vector $(1, \alpha)$ is zero, implying that m is constant in the direction of this vector, and thus

$$m(t,\nu) = m\left(t - \frac{\nu}{\alpha}, 0\right). \tag{7}$$

Combining equation (7) with the boundary condition (2), we can express the solution of the transport equation for large time t and all age ν as

$$m(t,\nu) = \frac{1}{\alpha} E\left(A\left(t - \frac{\nu}{\alpha} - T_p\right)\right). \tag{8}$$

We now express the levels of hemoglobin M and erythropoietin A in terms of a system of equations that does not depend explicitly on the partial differential equation (1). Integrating equation (1) over age ν and then using equation (8) we obtain a differential equation with two delays describing the time evolution of the level of hemoglobin:

$$\begin{aligned}\frac{dM(t)}{dt} &= -R\alpha\left(m\left(t,\nu_{\max}\right) - m\left(t,0\right)\right)\\ &= -R\left[E\left(A\left(t - T_{\mathrm{rbc}} - T_p\right)\right) - E\left(A\left(t - T_p\right)\right)\right],\end{aligned}$$

where

$$T_{\mathrm{rbc}} = \frac{\nu_{\max}}{\alpha} \tag{9}$$

is the lifespan of erythrocytes. Thus, together with equation (5), we describe the time evolution of the levels of hemoglobin and erythropoietin by the following non-linear system of ordinary differential equations:

$$\frac{dM(t)}{dt} = -R\left[E\left(A\left(t - T_{\mathrm{rbc}} - T_p\right)\right) - E\left(A\left(t - T_p\right)\right)\right] \tag{10a}$$

$$\frac{dA(t)}{dt} = -kA\left(t\right) + F(M(t)). \tag{10b}$$

3.2 Existence and uniqueness of steady state

We show existence of an equilibrium point of system (10) and verify its uniqueness.

Using the solution of the transport equation as expressed in equation (8) and applying a change of variables $\tau = \frac{\nu}{\alpha}$, we write equation (4) as

$$\begin{aligned} M(t) &= \frac{R}{\alpha}\int_0^{\nu_{\max}} E\left(A\left(t-\frac{\nu}{\alpha}-T_p\right)\right)\mathrm{d}\nu \\ &= R\int_0^{T_{\mathrm{rbc}}} E(A(t-\tau-T_p))\mathrm{d}\tau. \end{aligned} \tag{11}$$

Let us define the values of $M(t)$ and $A(t)$ at equilibrium as M_∞ and A_∞, respectively. To find an expression for the equilibrium values in terms of the reduced system, we let $M(t) = M_\infty$ and $A(t) = A_\infty$, also implying $\frac{dA(t)}{dt} = 0$. From equations (11) and (10b) we have

$$M_\infty = RT_{\mathrm{rbc}}E(A_\infty) \tag{12a}$$

$$0 = -kA_\infty + F(M_\infty). \tag{12b}$$

Solving equation (12b) for A_∞ and plugging the result back into equation (12a) we find

$$0 = RT_{\mathrm{rbc}}E\Big(\frac{1}{k}F(M_\infty)\Big) - M_\infty. \tag{13}$$

Every solution to this equation with respect to M_∞ gives an equilibrium point of the system. We see that the right hand side of equation (13) takes on a positive value when $M_\infty = 0$, is negative for large values of M_∞, and is a continuous function of M_∞. By the intermediate value theorem, equation (13) must have at least one positive solution. Furthermore, the right hand side of equation (13) is a monotone decreasing function, and so there exists a unique positive M_∞ such that equation (13) holds. Since A_∞ is a function of M_∞, we conclude that there is a unique equilibrium point (M_∞, A_∞) with both M_∞ and A_∞ positive.

3.3 Conditions for stability of the steady state

We study the behavior of the system (10) around the equilibrium point (M_∞, A_∞) through the roots of the characteristic equation, which we derive from the linearized system of equations around the equilibrium point. We linearize the system by calculating the first order Taylor expansions in the neighborhood of the equilibrium point for the functions E and F

$$\begin{aligned} E(s) &= E(A_\infty) + E'(A_\infty)(s-A_\infty) + O\left((s-A_\infty)^2\right) \\ F(s) &= F(M_\infty) + F'(M_\infty)(s-M_\infty) + O\left((s-M_\infty)^2\right). \end{aligned}$$

Thus, neglecting second and higher order terms, system (10) becomes

$$\frac{dM(t)}{dt} = -RE'(A_\infty)\left[\left[A(t-T_{\mathrm{rbc}}-T_p)-A_\infty\right]-\left[A(t-T_p)-A_\infty\right]\right] \tag{14a}$$

$$\frac{dA(t)}{dt} = -k\left(A(t)-A_\infty\right) + F'(M_\infty)\left(M(t)-M_\infty\right), \tag{14b}$$

where we used equation (12b) to get equation (14b). This system locally describes the time evolution of $(M(t), A(t))$ around the equilibrium point (M_∞, A_∞). We introduce perturbations from the stationary values

$$\tilde{M}(t) = M(t) - M_\infty$$
$$\tilde{A}(t) = A(t) - A_\infty.$$

Plugging these into system (14) we obtain

$$\frac{d\tilde{M}(t)}{dt} = -RE'(A_\infty)\left[\tilde{A}(t - T_{\mathrm{rbc}} - T_p) - \tilde{A}(t - T_p)\right] \tag{15a}$$
$$\frac{d\tilde{A}(t)}{dt} = -k\tilde{A}(t) + F'(M_\infty)\tilde{M}(t). \tag{15b}$$

We are interested in finding the characteristic values of this linearized system. We search for solutions of the form

$$\tilde{M}(t) = M_0 e^{\lambda t}$$
$$\tilde{A}(t) = A_0 e^{\lambda t},$$

where λ is the characteristic value of the system. Plugging this form of $\tilde{M}$ and $\tilde{A}$ into system (15), we arrive at the following homogeneous system of linear equations in (M_0, A_0):

$$\left(RE'(A_\infty)\left(e^{-\lambda T_{\mathrm{p}}} - e^{-\lambda(T_{\mathrm{p}}+T_{\mathrm{rbc}})}\right)\right)A_0 + (-\lambda)M_0 = 0$$
$$(\lambda + k)A_0 + \left(-F'(M_\infty)\right)M_0 = 0.$$

To find a non-trivial solution the determinant of the system has to be zero. This condition provides the characteristic equation associated with system (14),

$$\lambda^2 + k\lambda - RE'(A_\infty)F'(M_\infty)\left[e^{-\lambda T_{\mathrm{p}}} - e^{-\lambda(T_{\mathrm{p}}+T_{\mathrm{rbc}})}\right] = 0. \tag{17}$$

We note that, as a consequence of the two delays in the model, the characteristic equation is transcendental. The steady state of the linearized system is asymptotically stable if all solutions to the characteristic equation have negative real parts, and is unstable if there exists a solution with positive real part [17]. We are interested particularly in the loss of stability through Hopf bifurcations.

Hopf bifurcations occur in the system when a pair of complex eigenvalues crosses the imaginary axis. We therefore search for purely imaginary eigenvalues, i.e. those of the form $\lambda = i\omega$, $\omega \in \mathcal{R}$. Enforcing this form into equation (17) and using trigonometric identities we obtain

$$\begin{aligned} -\omega^2 + ik\omega = &\left[2RE'(A_\infty)F'(M_\infty)\sin\left(\omega\left(T_{\mathrm{p}} + \frac{T_{\mathrm{rbc}}}{2}\right)\right)\sin\left(\omega\frac{T_{\mathrm{rbc}}}{2}\right)\right] \\ &+ i\left[2RE'(A_\infty)F'(M_\infty)\cos\left(\omega\left(T_{\mathrm{p}} + \frac{T_{\mathrm{rbc}}}{2}\right)\right)\sin\left(\omega\frac{T_{\mathrm{rbc}}}{2}\right)\right]. \end{aligned} \tag{18}$$

We present three conditions to ensure that the complex numbers on either side of equation (18) are equal. Two conditions are to satisfy equal arguments of the complex numbers: first, we need that the ratios of the imaginary part over the real part of both sides are equal, and second, the real parts on both sides of (18) need to have the

same sign. Finally, the third condition is the requirement that the absolute values of both sides need to be equal. The three conditions are represented respectively by the following relations:

$$-\frac{\omega}{k} = \tan\left(\omega\left(T_{\mathrm{p}} + \frac{T_{\mathrm{rbc}}}{2}\right)\right) \tag{19a}$$

$$\sin\left(\omega\left(T_p + \frac{1}{2}T_{rbc}\right)\right)\sin\left(\omega\frac{T_{rbc}}{2}\right) > 0 \tag{19b}$$

$$\omega^4 + k^2\omega^2 = 4\left(RE'\left(A_\infty\right)F'\left(M_\infty\right)\right)^2\sin^2\left(\omega\frac{T_{\mathrm{rbc}}}{2}\right). \tag{19c}$$

We name equations (19a), (19b) and (19c) the argument equation, the sign condition and the modulus equation, respectively.

In the following section, we determine the regions of the parameter space for which all conditions in (19) are met, implying that there may exist a Hopf bifurcation in that region.

4 Bifurcation analysis

In this section, we study the conditions under which the model presented in Section 2 can reproduce a dynamical disease. We determine the instances where the equilibrium point loses stability through a Hopf bifurcation. A Hopf bifurcation occurs when a pair of complex conjugate eigenvalues of the system crosses the imaginary axis through the varying of one or more parameters [18,29]. In order to find Hopf bifurcations, we first find all purely imaginary solutions of the characteristic equation, i.e. when equations (19a) and (19c) have a solution simultaneously and condition (19b) is satisfied. We then verify that we indeed have Hopf bifurcations at these points.

If $\lambda = i\omega$ is a root of the characteristic equation, ω must satisfy equations (19a), (19b), and (19c). The possible values of ω that satisfy the argument equation (19a) are characterized in the following proposition.

Proposition 1 *(a) For each $\ell = 1, 2, \ldots$ there exists a unique $\omega_\ell > 0$ belonging to the interval*

$$\left]\frac{-\frac{\pi}{2} + \pi\ell}{T_p + \frac{1}{2}T_{\mathrm{rbc}}},\ \frac{\frac{\pi}{2} + \pi\ell}{T_p + \frac{1}{2}T_{\mathrm{rbc}}}\right[\tag{20}$$

such that ω_ℓ is a solution of the argument equation

$$\tan\left(\omega_\ell\left(T_{\mathrm{p}} + \frac{T_{\mathrm{rbc}}}{2}\right)\right) = -\frac{\omega_\ell}{k}. \tag{21}$$

(b) There are infinitely many solutions $\omega_\ell > 0$ to the argument equation such that the "sign condition" (19b) is satisfied.

Proof Straightforward.

Determining when ω satisfies the modulus equation is more involved. Let us re-write modulus equation (19c) as

$$-RE'\left(A_\infty\right)F'\left(M_\infty\right) = \frac{|w|\sqrt{w^2 + k^2}}{2|\sin(\omega\frac{T_{\mathrm{rbc}}}{2})|} \tag{22}$$

and define the function g as the right hand side of this equation

$$g(\omega) := \frac{|w|\sqrt{w^2+k^2}}{2|\sin(\omega\frac{T_{\text{rbc}}}{2})|}. \tag{23}$$

The left hand side of equation (22) is found in the characteristic equation (17) as the coefficient of a combination of exponential functions, the absolute value of which is bounded by 2 when λ is purely imaginary. We note that for imaginary λ, the term $|\lambda^2+\lambda k|$ in the characteristic equation can be arbitrarily large. As we wish to consider arbitrary values of $|\lambda|$, the named coefficient must be able to take on arbitrarily large values to fulfill the characteristic equation. Thus, we focus on the exponent r, as it is directly responsible for the speed of increase of this term. This exponent will act as the key parameter in the following analysis.

We express the left hand side of equation (22) as the function b depending on r.

$$b(r) = -RE'\left(A_\infty\right)F'\left(M_\infty\right). \tag{24}$$

As we have a large number of parameters in our model, we facilitate our analysis by introducing two strictly positive dimensionless parameters, P and Q:

$$P = \frac{G}{2E_{50}} \tag{25}$$

$$Q = \frac{D}{2F_{50}}, \tag{26}$$

where D and G are defined as the upper bounds of M_∞ and A_∞, respectively:

$$D = RT_{\text{rbc}}E_{\max} \tag{27}$$

$$G = \frac{F_{\max}}{k}. \tag{28}$$

We will use the dimensionless parameters P and Q to perform the bifurcation analysis. These allow a simple and precise description of the imaginary roots of the characteristic equation.

The next proposition determines the dependence of the equilibrium point on r.

Proposition 2 *The unique equilibrium point (M_∞, A_∞), defined by equations (12a) and (12b), can be expressed as*

$$M_\infty(r) = \frac{D}{2Q}\psi(r) \tag{29a}$$

$$A_\infty(r) = \frac{G}{1+\psi(r)^r}. \tag{29b}$$

where $\psi(r)$ is the unique positive solution of the equation $S(\psi)=0$, where

$$S(\psi) := \psi^{r+1} + (1+2P)\psi - 4PQ. \tag{30}$$

Proof Using equation (13) and the definition of P and Q, we obtain

$$\frac{1}{2P}M_\infty(r)^{r+1} + \left(1+\frac{1}{2P}\right)F_{50}^r M_\infty(r) - DF_{50}^r = 0. \tag{31}$$

We eliminate the constant F_{50} by introducing a dimensionless positive function $\psi(r)$:

$$\psi(r) := \frac{M_\infty}{F_{50}} = \frac{2Q}{D} M_\infty(r). \tag{32}$$

We substitute (32) into (31) and obtain

$$\Big(\frac{D}{2Q}\Big)^{r+1}\Big[\frac{1}{2P} S(\psi)\Big] = 0, \tag{33}$$

implying that $S(\psi) = 0$. As $S(0) = -4PQ < 0$ and

$$S(2Q) = 2^{r+1}Q^{r+1} + (1+2P)(2Q) - 4PQ = 2^{r+1}Q^{r+1} + 2Q > 0,$$

we see that there must exist at least one $\psi(r)$ such that $S(\psi) = 0$ with $0 < \psi(r) < 2Q$, and so there exists a solution to equation (30).

From

$$S'(\psi) = \frac{d}{d\psi} S(\psi) = (r+1)\psi^r + 1 + 2P, \tag{34}$$

we see that for $\psi \geq 0$, $S'(\psi) > 0$, and so the function $S(\psi)$ is strictly increasing for all $r \geq 1$. Therefore, we can conclude that $S(\psi) = 0$ has a unique positive solution. □

The following proposition shows the dependence of the left hand side of the modulus equation (22) on r.

Proposition 3 *The left term of modulus equation (22) can be expressed as*

$$b(r) = \frac{k}{T_{rbc}} \frac{r\psi(r)^{r+1}}{4PQ} = \frac{k}{T_{rbc}} r\Big(1 - \frac{(1+2P)\psi(r)}{4PQ}\Big). \tag{35}$$

Proof We consider the derivatives of E (see eq. (3)) and F (see eq. (6)):

$$F'(s) = -F_{\max} \frac{r F_{50}^r s^{r-1}}{(F_{50}^r + s^r)^2} \tag{36a}$$

$$E'(s) = E_{\max} \frac{E_{50}}{(E_{50} + s)^2}, \tag{36b}$$

and substitute into (24) to obtain

$$b(r) = \frac{k}{T_{rbc}} \frac{E_{50}}{(E_{50} + A_\infty)} \frac{M_\infty^r}{(F_{50}^r + M_\infty^r)} r. \tag{37}$$

We define f as

$$f(r) = \frac{E_{50}}{(E_{50} + A_\infty(r))} \frac{M_\infty^r(r)}{(F_{50}^r + M_\infty^r(r))} r \tag{38}$$

so that $b(r) = \frac{k}{T_{rbc}} f(r)$. Rewriting f as

$$f(r) = \frac{r}{1 + \frac{A_\infty}{E_{50}}} \frac{\Big(\frac{M_\infty}{F_{50}}\Big)^r}{1 + \Big(\frac{M_\infty}{F_{50}}\Big)^r}, \tag{39}$$

and using the following relations that follow from (25), (26), (29a) and (29b):

$$\frac{A_\infty(r)}{E_{50}} = \frac{2P}{1 + \psi(r)^r} \tag{40a}$$

$$\frac{M_\infty(r)}{F_{50}} = \psi(r), \tag{40b}$$

where $\psi(r)$ is the unique root of (30) as proved in Proposition 2, we have that

$$f(r) = \frac{r}{1+\frac{2P}{1+\psi(r)^r}} \frac{\psi(r)^r}{1+\psi(r)^r} = \frac{r\psi(r)^r}{1+2P+\psi(r)^r} = \frac{r\psi(r)^{r+1}}{(1+2P)\psi(r)+\psi(r)^{r+1}}. \quad (41)$$

From (30) we know that $\psi^{r+1} = 4PQ - (1+2P)\psi > 0$ and then

$$f(r) = \frac{r\psi(r)^{r+1}}{4PQ} = r\frac{4PQ-(1+2P)\psi(r)}{4PQ} = r\Big(1-\frac{(1+2P)\psi(r)}{4PQ}\Big). \quad (42)$$

Therefore (35) holds. □

Now that we have introduced some notation which facilitates our analysis of the imaginary roots of the characteristic equation, we separate the following analysis into two cases based on the value of r: $r = 1$ and $r > 1$. For the case $r = 1$, we show that there exists no possible solution for the modulus equation (19c). For $r > 1$, we partition the parameter space based on relations between the dimensionless parameters P and Q, and determine the conditions under which Hopf bifurcations occur within each subregion.

4.1 Bifurcation analysis for $r = 1$

Theorem 1 *For $r = 1$, there exists no possible solution for the modulus equation* (19c)*, implying that no Hopf bifurcations exist in this case.*

Proof Let us first look at the right hand side of the modulus equation (22). At $\omega = 0$, the function $g(\omega)$ (see (23)) has a removable discontinuity: $\lim_{\omega\to 0} g(\omega) = \frac{k}{T_{rbc}}$, and the infimum of $g(\omega)$ occurs in the limit as $\omega \to 0$:

$$\min_{\omega\geq 0} |g(\omega)| = lim_{\omega\to 0}\,|g\,(\omega)| = \frac{k}{T_{rbc}}.$$

Thus, $g(\omega_\ell) \geq \frac{k}{T_{rbc}}$ for each $\ell = 1, 2, \ldots$.

Now let us look at the left hand side of the modulus equation (22). From Proposition 3 we have that

$$b(1) = \frac{k}{T_{rbc}}\Big(1-\frac{(1+2P)}{4PQ}\psi(1)\Big) < \frac{k}{T_{rbc}}, \quad (43)$$

since P, Q and $\psi\,(1)$ are all positive.

Thus we see that the left hand side of (22) is always less than $\frac{k}{T_{rbc}}$, while the right hand side of (22) is always at least $\frac{k}{T_{rbc}}$, showing that the modulus equation (22) is never satisfied for $r = 1$. □

4.2 Bifurcation analysis for $r > 1$

We now consider the case $r > 1$. In the following, we divide the parameter space into three regions according to the dependence of the equilibrium point (M_∞, A_∞) on r. We define the nullcline where the derivative $M'_\infty(r)$ is identically zero, and the sub- and supercline where this derivative is negative and positive, respectively. Within each region, we determine the conditions for which there exists pure imaginary roots to the characteristic equation (17). Finally, we show that all such imaginary roots correspond to a loss of stability of the equilibrium point via a Hopf bifurcation.

4.2.1 Nullcline

Proposition 4 *In the nullcline the function $\psi(r)$ from Proposition 2 satisfies $\psi(r) = 1$ for all $r > 1$.*

Proof From Proposition 2 we have that $\psi(r)$ is the unique solution of $S(\psi) = 0$ (see eq. (30)). Computing the derivative of $S(\psi(r))$ with respect to r we have

$$(r+1)\psi^r \frac{d\psi}{dr} + \psi^{r+1}\log(\psi) + (1+2P)\frac{d\psi}{dr} = 0. \tag{44}$$

Isolating $\frac{d\psi}{dr}$ we obtain

$$\frac{d\psi}{dr} = -\frac{\psi^{r+1}\log(\psi)}{(r+1)\psi^r + 1 + 2P}. \tag{45}$$

From the definition of $M_\infty(r)$ in (29a) we have that if $M'_\infty(r) = 0$, then $\psi'(r) = 0$. Since $\psi \neq 0$, we have from (45) that $\log(\psi) = 0$, implying that $\psi(r) = 1$ for all $r > 1$. □

We characterize the nullcline of our parameter space in the following theorem.

Theorem 2 *For $r > 1$, $M'_\infty(r) = 0$ if and only if $Q = \frac{1+P}{2P}$.*

Proof First assume that $Q = \frac{1+P}{2P}$. From Proposition 2, $\psi(r) > 0$ is the unique positive solution of equation $S(\psi) = 0$, (see (30)). Plugging $Q = \frac{1+P}{2P}$ into $S(\psi)$ we obtain

$$\psi(r)^{r+1} + (1+2P)\psi(r) - 2(1+P) = 0.$$

It is immediately seen that $\psi(r) = 1$ is a solution of this equation. Then from equation (29a) we see that $M_\infty(r) = \frac{D}{2Q}$, i.e. $M_\infty(r)$ is a constant. Thus, $M'_\infty(r) = 0$.

Now assume that $M'_\infty(r) = 0$, i.e. we are on the nullcline. From Proposition 4 we know that $\psi(r) = 1$, for all $r > 1$ in the nullcline, and from Proposition 2 we know that $\psi(r)$ is the unique root of $S(\psi) = 0$. Substituting $\psi(r) = 1$ in $S(\psi) = 0$ we obtain

$$1^{r+1} + (1+2P) - 4PQ = 0.$$

Isolating Q, we obtain $Q = \frac{1+P}{2P}$. □

In the following, we identify the family of values of r where bifurcations can occur in the nullcline. Recall that there exists a sequence ω_ℓ, $\ell = 1, 2, \ldots$ which satisfies the argument equation stated in Proposition 1.

Theorem 3 *Let us assume $Q = \frac{1+P}{2P}$. Then, for every $\ell = 1, 2, \ldots$, the only values of r that solve the argument equation (19a) and the modulus equation (19c) are the exponents*

$$r_\ell^{null} := \frac{T_{rbc}}{k} g(\omega_\ell) 2(1+P). \tag{46}$$

This implies that Hopf bifurcations can only occur at these values of r.

Proof We assume that P and Q satisfy the nullcline condition, $Q = \frac{1+P}{2P}$, and consequently $\psi(r) = 1$, for all $r \geq 1$ from Proposition 4. From the expression of $b(r)$ in Proposition 3 we obtain that

$$b(r) = \frac{k}{T_{rbc}} \frac{r}{2(1+P)}.$$

Recall that $b(r)$ is the left hand side of the modulus equation (22). Evaluating the modulus equation (22) at the roots ω_ℓ of the argument equation (19a), we obtain

$$\frac{k}{T_{rbc}} \frac{r_\ell^{\text{null}}}{2(1+P)} = g(\omega_\ell),$$

and so r_ℓ^{null} satisfies (46). □

We have determined conditions for the existence of imaginary roots to the characteristic equation in the nullcline. In the following sections we perform a similar analysis for the subcline and the supercline.

4.2.2 Subcline

Recall that we define the subcline as the region of the parameter space for which $M'_\infty(r) < 0$.

Proposition 5 *We are on the subcline, i.e. $M'_\infty(r) < 0$, if and only if $Q > \frac{1+P}{2P}$.*

Proof This proof is analogous to the proof of Theorem 2.

If $Q > \frac{1+P}{2P}$ then $S(1) < 0$ and so $1 < \psi(r)$. Since $\psi(r) > 1$, equation (45) implies that $\frac{d\psi}{dr} < 0$ and from the definition of $M_\infty(r)$ in Proposition 2 we conclude that $M'_\infty(r) < 0$.

Conversely, suppose $M'_\infty(r) < 0$. Then from the definition of $M_\infty(r)$ in Proposition 2 we have that $\frac{d\psi}{dr} < 0$. Equation (45) then implies that $\psi(r) > 1$, which then means that $S(1) < 0$, which is equivalent to $Q > \frac{1+P}{2P}$. □

Let us define the set of values $r_\ell^{\text{sub}} > 1$ such that both the modulus equation and the argument equation are satisfied in the subcline. Recall again that there exists a sequence ω_ℓ, $\ell = 1, 2, \ldots$ which satisfies the argument equation stated in Proposition 1.

Theorem 4 *In the subcline, there exists a sequence of exponents r_ℓ^{sub} for which the modulus equation (19c) and the argument equation (19a) are satisfied simultaneously. That is, there exists a unique $r_\ell^{sub} > 1$ for every $\ell = 1, 2, \ldots$ such that*

$$b(r_\ell^{sub}) = g(\omega_\ell). \tag{47}$$

Proof Since $b(r) > 0$ and from Proposition 2 we know that $\psi(r) > 0$, it follows from equation (35) in Proposition 3 that

$$0 < \frac{(1+2P)\psi(r)}{4PQ} < 1.$$

This provides a sharper estimate for the upper bound of ψ:

$$0 < \psi < \frac{4PQ}{(1+2P)} = 2Q\frac{2P}{1+2P} < 2Q.$$

The derivative of $b(r)$ with respect to r is

$$b'(r) = \frac{k}{T_{rbc}}\left[\Big(1 - \frac{1+2P}{4PQ}\psi(r)\Big) - r\frac{1+2P}{4PQ}\psi'(r)\right]. \tag{48}$$

From Proposition 5 we have that $\psi'(r) < 0$. Therefore from (48) we have that $b'(r) > 0$ for all $r \geq 1$ and thus $b(r)$ will be strictly increasing for $r > 1$. Since $\psi(r)$ is strictly decreasing, we also have that the function $1 - \frac{1+2P}{4PQ}\psi(r)$ is strictly increasing. From here we have that

$$\min_{r\geq 1}\Big(1 - \frac{1+2P}{4PQ}\psi(r)\Big) = 1 - \frac{1+2P}{4PQ}\psi(1) = \frac{\psi(1)^2}{4PQ},$$

where we used that ψ satisfies $S(\psi) = 0$ (see (30)). Therefore

$$0 < \frac{\psi(1)^2}{4PQ} < 1 - \frac{1+2P}{4PQ}\psi(r), \tag{49}$$

for all $r > 1$. Multiplying the inequality (49) by r and $\frac{k}{T_{rbc}}$ we obtain

$$\frac{k}{T_{rbc}}\frac{\psi(1)^2}{4PQ}r < \frac{k}{T_{rbc}}r\Big(1 - \frac{1+2P}{4PQ}\psi(r)\Big) = b(r).$$

From this we see that $\lim_{r\to\infty} b(r) = +\infty$, implying that $b(r)$ may take on any value larger than $b(1)$. Since $b(r)$ is strictly increasing, there exists a unique $r_\ell^{\text{sub}} > 1$ for every $\ell = 1, 2, \ldots$ such that equation (47) is satisfied. □

4.2.3 Supercline

Recall that we define the supercline as the region of the parameter space for which $M'_\infty(r) > 0$.

Proposition 6 *We are on the supercline, i.e. $M'_\infty(r) > 0$, if and only if $Q < \frac{1+P}{2P}$.*

Proof This proof is analogous to the proof of Theorem 2 and Proposition 5.

If $Q < \frac{1+P}{2P}$ then $S(1) > 0$ and so $1 > \psi(r)$. Since $\psi(r) < 1$, equation (45) implies that $\frac{d\psi}{dr} > 0$ and from the definition of $M_\infty(r)$ in Proposition 2 we conclude that $M'_\infty(r) > 0$.

Conversely, suppose $M'_\infty(r) > 0$. Then from the definition of $M_\infty(r)$ in Proposition 2 we have that $\frac{d\psi}{dr} > 0$. Equation (45) then implies that $\psi(r) < 1$, which then means that $S(1) > 0$, which is equivalent to $Q < \frac{1+P}{2P}$. □

In the following proposition, we divide the supercline into two subregions with different behaviors.

Proposition 7 *Let us assume we are in the supercline region, that is, $Q < \frac{1+P}{2P}$. We set $\beta = \frac{1+2P}{4PQ}$. Then,*

(a) If $\beta \leq 1$ then $\lim_{r\to\infty} b(r) = +\infty$.
(b) If $\beta > 1$ then $\lim_{r\to\infty} b(r) = 0$.

Proof (a) From Proposition 3 we have that

$$0 < b(r) = \frac{k}{T_{rbc}} r(1 - \beta\psi(r)) \tag{50}$$

and from Proposition 6 we have that $\psi(r) < 1$. This immediately implies that

$$b(r) > \frac{k}{T_{rbc}} r(1 - \beta),$$

so for $\beta < 1$, this implies that $\lim_{r\to\infty} b\,(r) = +\infty$.

In the case of $\beta = 1$, the above argument is insufficient to show that $\lim_{r\to\infty} b\,(r) = +\infty$, which, by (50), is equivalent to $\lim_{r\to\infty} r\,(1 - \psi\,(r)) = +\infty$. Suppose on the contrary that $c := \liminf_{r\to\infty} r\,(1 - \psi\,(r)) < \infty$. Then there exists a sequence $\left\{r_j\right\}_{j=1}^{\infty}$ such that $\lim_{j\to\infty} r_j = \infty$ and $r_j\left(1 - \psi\left(r_j\right)\right) < 2c$ for all j, i.e.,

$$\psi\left(r_j\right) > 1 - \frac{2c}{r_j}$$

for all j. Then, using the fact that $1 + 2P = 4PQ$ because $\beta = 1$, we have

$$\liminf_{j\to\infty} S\left(\psi\left(r_j\right)\right) \geq \liminf_{j\to\infty} \left[\left(1 - \frac{2c}{r_j}\right)^{r_j+1} + (1 + 2P)\left(1 - \frac{2c}{r_j}\right) - 4PQ\right] = e^{-2c} > 0.$$

But this implies that $S\left(\psi\left(r_j\right)\right) > 0$ for large enough j, which is a contradiction, since ψ is a root of S, i.e. $S\left(\psi\left(r_j\right)\right) = 0$ for all j.

(b) We have

$$b(r) = \frac{k}{T_{rbc}} r(1 - \beta\psi(r)) = \frac{k}{T_{rbc}} \frac{r\psi(r)^{r+1}}{4PQ}.$$

From the definition of function $S(\psi)$ in equation (30) in Proposition 2 we have that $S(\frac{1}{\beta}) > 0$, and for every $r > 1$, $0 < \psi(r) < \frac{1}{\beta}$. Consequently

$$0 < b(r) < \frac{k}{4T_{rbc}PQ} r\big(\frac{1}{\beta}\big)^{r+1},$$

and so $\lim_{r\to\infty} b(r) = 0$. □

Let us remark that $\frac{1+2P}{4P} < \frac{1+P}{2P}$. In addition, if $Q < \frac{1+P}{2P}$ then $\beta \leq 1$ if and only if $\frac{1+2P}{4P} \leq Q < \frac{1+P}{2P}$. On the other hand, $\beta > 1$ if and only if $Q < \frac{1+2P}{4P}$.

Theorem 5 *Assume $\frac{1+2P}{4P} \leq Q < \frac{1+P}{2P}$ (i.e. $\beta \leq 1$). For each $\ell = 1, 2, \ldots$, there exists a unique $r_\ell^{sup} > 1$ satisfying the argument equation (19a) and the modulus equation (19c) simultaneously*

$$b(r_\ell^{sup}) = g(\omega_\ell). \tag{51}$$

Proof From Proposition 7(a), since $\beta \leq 1$, $\lim_{r\to\infty} b(r) = \infty$. Therefore $b(r)$ attains any real value larger that $b(1)$. □

Theorem 6 *For $Q < \frac{1+2P}{4P}$ (i.e. $\beta > 1$) there exist at most a finite number of exponents r_ℓ^{sup} associated to the corresponding $\omega_\ell > 0$, $\ell = 1, 2, \ldots$, satisfying the argument equation (19a) and modulus equation (19c) simultaneously*

$$b(r_\ell^{sup}) = g(\omega_\ell). \tag{52}$$

Proof From Proposition 7(b), we have $\lim_{r\to\infty} b(r) = 0$ since $\beta > 1$. Therefore the function $b\,(r)$ attains its maximum for some $r_0 \in [1, +\infty[$. □

We have identified all possible pure imaginary roots $\lambda = i\omega$ to the characteristic equation. To ensure that the equilibrium loses stability through a Hopf bifurcation at these points, the roots must cross the imaginary axis. In the following section, we show that all imaginary roots in our system define Hopf points.

4.2.4 Existence of Hopf points

Recap: In Section 3, we defined three conditions for the existence of purely imaginary roots of the characteristic equation (17). We have shown that there is an increasing sequence of frequencies $\omega_\ell > 0, \ell = 1, 2, \ldots$ for which the argument equation (19a) is satisfied and the sign condition (19b) holds. These frequencies depend only on $T_p > 0$, $T_{rbc} = \frac{\nu_{\max}}{\alpha} > 0$, and $k > 0$.

Fulfilling the third condition, the modulus equation (19c), is more involved. To facilitate the analysis we introduced three dimensionless parameters: P, Q and $r \geq 1$.

For $r = 1$, we showed that the modulus equation is never satisfied and therefore there exist no purely imaginary roots to the characteristic equation. For $r > 1$, we define three regions with distinct properties on the first quadrant of the (P, Q) plane, namely the nullcline, subcline and supercline.

The nullcline consists of the set of points (P, Q) belonging to the positive branch of $Q = \frac{1+P}{2P}$ with asymptotes $Q = \frac{1}{2}$ and $P = 0$. In the nullcline, we establish explicit formulas for the exponents $r_\ell > 1$ for which the modulus equation is satisfied and therefore $\lambda = i\omega_\ell$ are purely imaginary roots of the characteristic equation.

The subcline consists of the set of points (P, Q) such that $Q > \frac{1+P}{2P}$. We show the existence of a unique sequence of values $r_\ell > 1$ such that $\lambda = i\omega_\ell$ is a root of the characteristic equation.

The supercline consists of the set of points (P, Q) such that $Q < \frac{1+P}{2P}$. We consider two subregions in this region. For $\frac{1+P}{4P} \leq Q < \frac{1+P}{2P}$, we obtain a similar result as the one for the subcline for the existence of a unique sequence of values $r_\ell > 1$. For $Q < \frac{1+P}{4P}$, we prove that there exist at most a finite number of solutions of the characteristic equation.

In the following, we show that all purely imaginary roots $\lambda = i\omega_\ell$ define Hopf bifurcations. This implies that the equilibrium point (M_∞, A_∞) changes stability from being spirally stable to being repellent.

Theorem 7 *A Hopf bifurcation occurs for each of the pure imaginary roots of the characteristic equation, that is, there exists a small neighborhood of a critical value $r = r_\ell > 1$ such that when $|r - r_\ell| < \epsilon$, $\epsilon < 1$, the real part of the root of the characteristic equation changes sign, i.e., the root crosses the imaginary axis.*

Proof We consider here only the case of the nullcline (where we have explicit expressions for $r_\ell > 0$). This analysis can be extended easily to the other regions.

Recall the characteristic equation

$$0 = \lambda^2 + k\lambda - RE'(A_\infty)\,F'(M_\infty)\left[e^{-\lambda T_{\rm p}} - e^{-\lambda(T_{\rm p}+T_{\rm rbc})}\right]$$

and let $\lambda = \eta + i\omega$ with η, $\omega \in \mathbf{R}$.

We define

$$L := -RE'(A_\infty)\,F'(M_\infty)$$

and consider the case of the nullcline, when

$$L = L(r) := \frac{k}{T_{\rm rbc}}\frac{r}{2(1+P)}, \qquad r \geq 1$$

Equating real and imaginary parts we have the equations

$$\eta^2 - \omega^2 + k\eta + Le^{-\eta T_p}(\cos\theta - e^{-\eta T_{\rm rbc}}\cos\phi) = 0 \tag{53}$$

$$(2\eta + k)\omega + Le^{-\eta T_p}(e^{-\eta T_{\rm rbc}}\sin\phi - \sin\theta) = 0 \tag{54}$$

where $\theta = \omega T_p$ and $\phi = \omega(T_p + T_{\rm rbc})$.

From

$$X := \cos\theta - \cos\phi = 2\sin\Big(\frac{\phi+\theta}{2}\Big)\sin\Big(\frac{\phi-\theta}{2}\Big)$$

$$Y := \sin\phi - \sin\theta = 2\cos\Big(\frac{\phi+\theta}{2}\Big)\sin\Big(\frac{\phi-\theta}{2}\Big),$$

we have that

$$\begin{aligned}\cos\theta - e^{-\eta T_{\rm rbc}}\cos\phi &= \cos\theta - \cos\phi + \cos\phi(1 - e^{-\eta T_{\rm rbc}}) \\ &= X + \cos\phi(1 - e^{-\eta T_{\rm rbc}})\end{aligned}$$

and

$$\begin{aligned}e^{-\eta T_{\rm rbc}}\sin\phi - \sin\theta &= (e^{-\eta T_{\rm rbc}} - 1)\sin\phi + \sin\phi - \sin\theta \\ &= Y - (1 - e^{-\eta T_{\rm rbc}})\sin\phi.\end{aligned}$$

Thus equations (53) and (54) can be rewritten as

$$L = e^{\eta T_p}\frac{\omega^2 - \eta^2 - k\eta}{X + \cos\phi(1 - e^{-\eta T_{\rm rbc}})} \tag{55}$$

$$L = e^{\eta T_p}\frac{(k+2\eta)\omega}{Y - (1 - e^{-\eta T_{\rm rbc}})\sin\phi}. \tag{56}$$

Since $\omega^2 > 0$, there exists an $\epsilon > 0$ such that $|\eta| \leq \epsilon$ implies $\omega^2 - \eta^2 - k\eta > 0$. Let us consider equation (55) for $|\eta| \leq \epsilon$ and $\omega \in]\omega_\ell - \gamma, \omega_\ell + \gamma[$, for small $\gamma > 0$.

For $\eta = 0$ and $\omega = \omega_\ell$ the following equation is satisfied

$$L(r_\ell^*) = \frac{k}{T_{\rm rbc}}\frac{r_\ell^*}{2(1+P)} = \frac{w_\ell^2}{X_0} > 0$$

where

$$X_0 = X(\omega_\ell) = 2\sin(\omega_\ell(T_p + \frac{1}{2}T_{\rm rbc}))\sin(\frac{\omega_\ell}{2}T_{\rm rbc}) > 0$$

is the sign condition (equation (19b)).

We consider the right-hand side of equation (55) for $w = w_\ell$ and $|\eta| \leq \epsilon$ as a function of η:

$$h(\eta) := e^{\eta T_p} \frac{\omega^2 - \eta^2 - k\eta}{X_0 + \cos\phi_\ell (1 - e^{-\eta T_{\rm rbc}})} \tag{57}$$

where $\phi_\ell = \omega_\ell (T_p + T_{\rm rbc})$.

Since $L(r) = \frac{k}{T_{\rm rbc}} \frac{r}{2(1+P)}$ we can write r as a function of η

$$r = r(\eta) = \frac{2(1+P)}{k} T_{\rm rbc} h(\eta).$$

We show that the behavior of r with respect to η for $|\eta| \leq \epsilon$ depends on the sign of $h'(0)$. Differentiating equation (57) and computing $h'(0)$ we can see that if $h'(0) < 0$ (and $h'(0) > 0$ respectively) there exists an $\epsilon_0 < \epsilon$ such that $h'(\eta) < 0$ (and $h'(\eta) > 0$ respectively) for $|\eta| \leq \epsilon_0$ since $h(\eta)$ is continuous in a neighborhood of 0. For singular values $h'(0)$ might vanish depending on the values of ω_ℓ, T_p and $T_{\rm rbc}$.

Thus $r(\eta)$ is strictly increasing for $|\eta| \leq \epsilon_0$ if $h'(0) > 0$ and strictly decreasing if $h'(0) < 0$. Therefore η changes sign when perturbing r around $r = r_\ell^*$ and so that in both cases the bifurcation at $\eta = 0$ results in a change of stability of the equilibrium. □

5 Examples of Hopf bifurcations and simulations

In this section we provide examples of Hopf bifurcations. We use parameters (shown in Table 2) which reproduce results within physiological ranges of hemoglobin and erythropoietin [9,10,24,26]. As the dynamics that results from supercritical Hopf bifurcations is oscillatory in nature, the goal of this approach is to study how the model can reproduce behavior characteristic to that of a dynamical hematological disease.

As hematological pathology is often associated with a change in the turnover rate of red blood cells, we consider examples varying α in the interval $[1, 5]$, a range larger by a factor of two that would be expected for healthy individuals. An example could be the oscillatory dynamics in levels of erythropoietin and hemoglobin often seen in patients with renal failure who are treated with erythropoiesis-stimulating agents (ESAs), which act on the longevity of red blood cells [11]. We then choose three different values of α from which we can calculate $T_{\rm rbc}$ using expression (9). Together with the values of T_p and k we use a bisection method to solve equation (21) for $l = 1$ and obtain ω_1.

Each α places us in a different region of the parameter space. In order to determine the region represented by each α, we compare P and Q, where a value of Q equal to, greater than, or less than $\frac{1+P}{2P}$ places us in the nullcline, subcline, or supercline, respectively. We compute the values of these parameters from expressions (25) and (26) using the definitions of D (see equation (27)) and G (see equation (28)). We calculate critical values of r where a Hopf bifurcation arises in each of the regions. We compute these critical values of r from expressions (46), (47), or (51) from Theorems 3, 4, or 5, respectively, depending on whether we are in the nullcline, subcline, or supercline.

In Table 3, we show results obtained for values of α corresponding to the nullcline, subcline, and supercline, respectively. We observe that for the given parameter values in Table 2 and any value of α, $P = 0.34$ remains constant and so $\frac{1+P}{2P} = 1.97058$ is constant as well. On the other hand, as Q depends on α, it varies in the interval

Table 2 Typical values of the parameters of the model

$\nu_{\max}$	120 days
k	2 day^{-1}
R	$3.0 \cdot 10^{-11}$ g
$E_{\max}$	$6 \cdot 10^{10}$ 1/(l · day)
E_{50}	50U/l
$F_{\max}$	68U/(l · day)
F_{50}	15g/l
T_{p}	12 days

Table 3 Results for three regions of the parameter space

α	P	Q	Region	ω_1	r_1	M_∞	A_∞
3.6537	0.34	1.97058	nullcline	0.10862	4.89839	15	17
3.1	0.34	2.32258	subcline	0.09862	4.63712	15.88188	14.76133
5	0.34	1.44	supercline	0.12823	6.79943	13.51835	22.7724

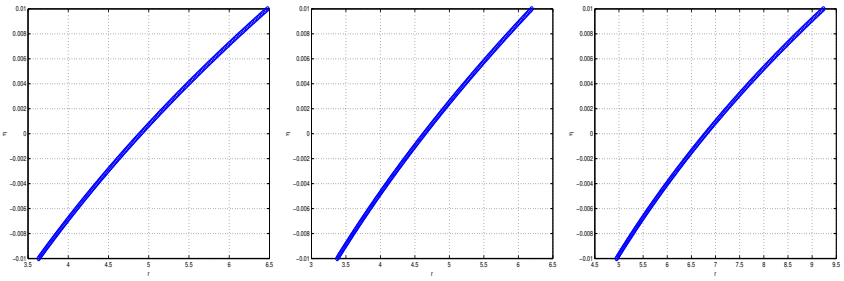

Fig. 1 Values of η, the real part of the complex root of the characteristic equation, as a function of r in an interval containing the critical value r_1. From left to right: nullcline, subcline and supercline cases.

$[1.4, 7.2]$ for the given interval of α, therefore placing us in different regions of the parameter space. Each pair $(\omega_1,\ r_1)$ satisfies the argument and modulus equations, (19a) and (19c), respectively, for purely imaginary roots of the characteristic equation.

As stated in Theorem 7, we expect a change of behavior in the evolution of the system's dynamics when varying the value of parameter r around the critical value r_1. We study this behavior numerically by looking for complex solutions to the characteristic equation, $\lambda = \eta + i\omega_1$, fixing the value of ω_1 as in Table 3. We compute the solutions for a range of r values around the corresponding critical values r_1 in each region in Table 3.

Figure 1 displays the values of η, the real part of the rightmost root of the characteristic equation, as a function of r. The pictures, from left to right, show how η varies for the nullcline case for $r \in [3.5, 6.5]$ $(r_1 = 4.89839)$, the subcline case for $r \in [3, 6.5]$ $(r_1 = 4.63712)$, and the supercline case for $r \in [4.5, 9.5]$ $(r_1 = 6.79943)$.

From Figure 1, we observe in each case that for values of $r < r_1$ the characteristic equation is only satisfied for negative η values, implying that the equilibrium point is spirally stable. Since the roots of the characteristic equation never cross the imaginary axis for $r = 1$, this implies that all eigenvalues of system (10) will have negative real part for any choice of parameter values. Thus, the steady state (12) is asymptotically

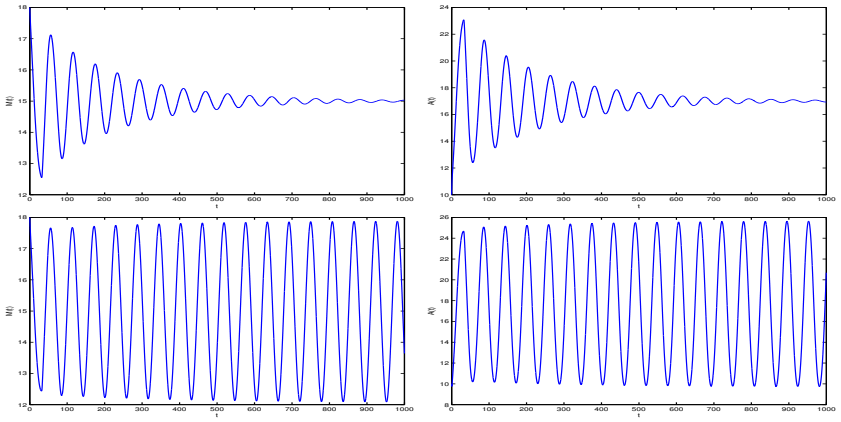

Fig. 2 Evolution of hemoglobin and erythropoietin until time $t = 1000$ for the nullcline case. Top: convergence to the equilibrium point for $r = 4.2 < 4.89839 = r_1$. Bottom: convergence to a limit cycle for $r = 5.2 > 4.89839 = r_1$.

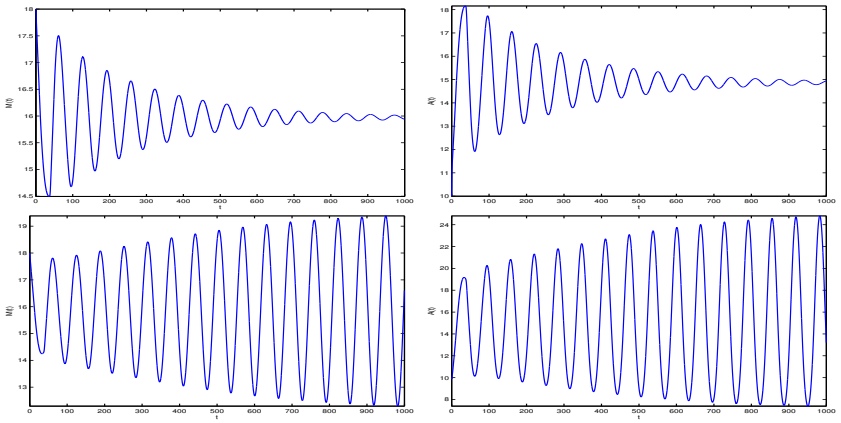

Fig. 3 Evolution of hemoglobin and erythropoietin until time $t = 1000$ for the subcline case. Top: convergence to the equilibrium point for $r = 4 < 4.63712 = r_1$. Bottom: convergence to a limit cycle for $r = 5 > 4.63712 = r_1$.

stable for any choice of parameters when $r = 1$ [17]. For $r > r_1$, the characteristic equation is only satisfied for positive η values, implying that the equilibrium point loses stability, repelling all trajectories to a stable limit cycle. Since the slope of η as a function of r in each case is positive at the critical r_1, we have that the Hopf bifurcations are supercritical [8].

Next, we illustrate this behavior by simulating the long term dynamics of the model for the presented values. We examine the evolution of the levels of hemoglobin $M(t)$ and erythropoietin $A(t)$ in the three regions until time $t = 1000$ days for the same initial values of $M(t)$ and $A(t)$.

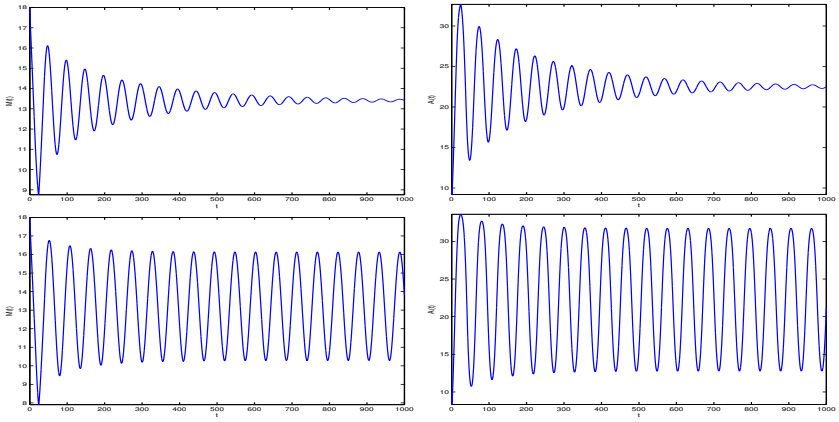

Fig. 4 Evolution of hemoglobin and erythropoietin until time $t = 1000$ for the supercline case. Top: convergence to the equilibrium point for $r = 6 < 6.79943 = r_1$. Bottom: convergence to a limit cycle for $r = 7 > 6.79943 = r_1$.

We display three figures, one for each region of the parameter space. In each, we present the long term dynamics of the model for some $r < r_1$ and $r > r_1$. The top of Figure 2 displays results in the nullcline for $r = 4.2$, showing the trajectories converging to the stable equilibrium point. The bottom of Figure 2 shows periodic behavior resulting from a Hopf bifurcation in the nullcline for $r = 5.2$. Figure 3 displays similar behavior in the subcline. The top picture shows a stable, attracting equilibrium point for $r = 4$ while the bottom picture shows trajectories which converge to a stable limit cycle with positive amplitude after the emergence of a Hopf bifurcation for $r = 5$. Similarly, in the supercline case in Figure 4, we observe the stable equilibrium point for $r = 6$ attracting all trajectories in the top picture and the formation of a stable limit cycle resulting from a Hopf bifurcation for $r = 7$.

We have given examples showing that for $\ell = 1$, $\omega_1 > 0$ gives a root of the argument equation satisfying the sign condition, and we can compute a unique exponent $r_1 > 1$ at which a supercritical Hopf bifurcation occurs. The real part of the root of the characteristic equation is positive for $r > r_1$, and therefore the equilibrium point becomes unstable and a stable limit cycle emerges, its amplitude increasing with r. All trajectories starting near the equilibrium point are attracted to the limit cycle. In all three cases, for $r < r_1$ the equilibrium point is spirally stable and attracts all trajectories.

6 Conclusions

Periodic diseases can be simulated by systems in which the equilibrium point loses stability through a Hopf bifurcation. In a model of erythropoiesis, this would result in oscillations in erythropoietin and hemoglobin levels. Clinically, such behavior is observed in patients who use erythropoiesis-stimulating agents (ESAs) after renal failure.

The goal of this paper was to provide a clearer understanding of the dynamics of an age-structured model of erythropoiesis through a theoretical bifurcation analysis.

We have reduced the model presented in Section 2 to a system of nonlinear ordinary differential equations with two constant delays and determined the conditions under which the unique equilibrium point can lose stability. We have performed a complete bifurcation analysis and derived analytical expressions which allow the identification of all Hopf bifurcations that occur over the parameter space. We have presented examples and shown through a numerical analysis of the roots of the characteristic equation that the Hopf bifurcations in our system are supercritical, implying long-term oscillations in hemoglobin and erythropoietin levels. Numerical simulations are in agreement with our analysis, showing the existence of oscillatory dynamics in both erythropoietin and hemoglobin levels for long time computations.

Acknowledgements This research has been motivated and partially supported by NSF via the Institute for Pure and Applied Mathematics (UCLA) program "Research in Industrial Projects for Students" 2008 and AMGEN Corporation in California. The authors thank students Raphiel Murden and David Pinney at RIPS 2008 as well as IPAM for their support. Special thanks to David Balaban and Gilles Gnacadja from AMGEN Corporation for their advice and helpful discussions.

First author acknowledges financial support by projects MICINN "Programa Ramon y Cajal" and MTM2008-03597.

References

1. Adimy M, Crauste F. Mathematical model of hematopoiesis dynamics with growth factor–dependent apoptosis and proliferation regulations. *Math. and Comp. Mod.*, 49(11–12):2128–2137, 2009.
2. Adimy M, Crauste F, Hbid ML, Qesmi, R. Stability and Hopf bifurcation for a cell population model with state-dependent delay. *SIAM J.Appl. Math.*, 70(5):1611–1633, 2010.
3. Adimy M, Crauste F, Marquet C. Asymptotic behavior and stability switch for a mature-immature model of cell differentiation, *Non. Lin. Anal. Real World Appl.*, 11(4):2913–2929, 2010.
4. Bélair J, Campbell SA. Stability and bifurcations of equilibria in a multiple-delayed differential equation. *SIAM J. Appl. Math.*, 54(5):1402–1424, 1994.
5. Bélair J, Mackey MC, Mahaffy JM. Age-structured and two-delay models for erythropoiesis. *Math. Biosci.*, 128(1–2):317–346, 1995.
6. Bernard S, Bélair J, Mackey MC. Oscillations in cyclical neutropenia: new evidence based on mathematical modeling. *J. Theor. Biol* 223:283–298, 2003.
7. Cornish-Bowden, A. *Fundamentals of enzyme kinetics*. Portland Press London, 2004.
8. Diekmann O, van Gils SA, Verduyn Lunel SM, Walther H-O. *Delay equations. Functional-, Complex-, and Nonlinear Analysis*. Applied Mathematical Sciences 110, New York, Springer-Verlag, 1995.
9. Erslev AJ. Erythrokinetics, in *Hematology*, McGraw-Hill, New York, pp. 414–442, 1990.
10. Erslev AJ. Erythropoietin titers in health and disease. *Semin. Hematol.* 28(Suppl. 3):2–8, 1991.
11. Fishbane S and Berns JS. Evidence and implications of haemoglobin cycling in anaemia management. *Nephrol Dial Transplant* 22: 2129-2132, 2007.
12. Foley C, Mackey MC. Dynamic hematological disease: a review. *J. Math. Biol.* 58(1):285–322, 2009.
13. Glass L, Mackey MC. *From Clocks to Chaos: The Rhythms of Life*. Princeton University Press, 1988.
14. Graber S, Krantz S. Erythropoietin and the control of red cell production. *Ann. Rev. Med.* 29:51–66, 1978.
15. Grodins FS, Gray JS Schroeder KR, Norins AL, and Jones RW. Respiratory responses to CO2 inhalation: a theoretical study of a nonlinear biological regulator. *J. Appl. Physiol.* 7(3):283–308, 1954.
16. Guevara MR, Glass L. Phase Locking, Period Doubling Bifurcations and Chaos in a Mathematical Model of a Periodically Driven Oscillator: A Theory for the Entrainment of Biological Oscillators and the Generation of Cardiac Dysrhythmias. *J. Math. Biol.* 14(1):1–23, 1982.

17. Hale JK, Verduyn Lunel, SM. *Introduction to Functional Differential Equations*. Applied Mathematical Sciences 99, New York, Springer-Verlag, 1993.
18. Kuznetsov YA. *Elements of Applied Bifurcation Theory*. Springer, 2004.
19. Mackey MC. Unified Hypothesis for the Origin of Aplastic Anemia and Periodic Hematopoiesis. *Blood*, 51(5):941–956, 1978.
20. Mackey MC. Periodic auto-immune hemolytic anemia: An induced dynamical disease. *Bull. Math. Biol.* 41(6):829–834, 1979.
21. Mackey MC, Glass L. Oscillation and chaos in physiological control systems. *Science*, 197(4300):287–289, 1977.
22. Mackey MC, Glass L. Complex Dynamics and Bifurcations in Neurology. *J. Theor. Biol.* 138:129–147, 1989.
23. Mahaffy JM, Bélair J, Mackey MC. Hematopoietic Model with Moving Boundary Condition and State Dependent Delay: Applications in Erythropoiesis. *J. Theor. Biol.* 190(2):135–146, 1998.
24. Miller CB, Jones RJ, Piantadosi S, Abeloff MD, Spivak JL. Decreased Erythropoietin Response in Patients with the Anemia of Cancer. *N. Engl. J. Med.* 332(24):1689–1692, 1990.
25. Milton JG, Mackey MC. Periodic haematological diseases: mystical entities or dynamical disorders? *J. R. Coll. Physicians Lond.* 23(4):236–241, 1989.
26. Orr JS, Kirk J, Gray KG, Anderson JR. A study of the interdependence of red cell and bone marrow stem cell populations. *Br. J. Haematol.* 15(1):23–34, 1968.
27. Pujo-Menjouet L, Mackey MC. Contribution to the study of periodic chronic myelogenous leukemia. *C. R. Biologies* 327:235–244, 2004.
28. Reimann HA. Periodic Diseases. *The Lancet*, 282(7311):782–782, 1963.
29. Strogatz SH. *Nonlinear Dynamics And Chaos*. Westview, 2000.